Ceramics-Silikáty 66 (3), 347-353 (2022)
www.ceramics-silikaty.cz doi: 10.13168/cs.2022.0030

IN VITRO DEGRADATION AND BIOACTIVITY OF ANTIBACTERIAL CHROMIUM DOPED β-TRICALCIUM PHOSPHATE BIOCERAMICS

#AMMAR Z. ALSHEMARY*,**, YASSER MUHAMMED***, NADER A. SALMAN****, RAFAQAT HUSSAIN*****, ALI MOTAMENI******, RIZA GÜRBÜZ******, MOHAMMED HLIYIL HAFIZ ALKAABI*******, AHMAD ABDOLAHI********

**Biomedical Engineering Department, Al-Mustaqbal University College, Hillah, Babil 51001, Iraq*
***Department of Chemistry, Faculty of Science, Universiti Teknologi Malaysia, 81310 UTM Skudai, Johor Darul Ta'zim, Malaysia*
****Aeronautical Techniques Engineering, AL-Farahidi University, Baghdad, Iraq*
*****Department of Medical Laboratory Techniques, Al-Manara College for Medical Sciences, Maysan, 62001, Iraq*
******Department of Chemistry, COMSATS University Islamabad, Park Road, Islamabad, 45550, Pakistan*
*******Department of Metallurgical and Materials Engineering, Middle East Technical University, Ankara, 06800, Turkey*
********College of Oil and Gas Engineering, Basrah University for Oil and Gas, Iraq*
*********Faculty of Mechanical Engineering, Universiti Teknologi Malaysia, 81310 UTM Johor Bahru, Johor, Malaysia*

#E-mail: ammar.zeidan@mustaqbal-college.edu.iq

Submitted May 14, 2022; accepted June 27, 2022

Keywords: β-tricalcium phosphate; Chromium; Microstructure; Bioactivity; Antibacterial

This study successfully incorporated different chromium ions (Cr^{3+}) fractions into β-tricalcium phosphate (βTCP) using the wet-precipitation process aided by microwave radiation. The microstructure analysis of the prepared materials was investigated using XRD and FESEM. The XRD results revealed that the characteristic peaks of Cr-βTCP materials matched the standard phase of βTCP crystals. The lattice parameters were decreased with increasing amounts of Cr^{3+} ions while the degree of crystallinity was increased. The FESEM results revealed that the entire materials were spherical from nano to micro size. The particle growth rate increased significantly as the amount of Cr^{3+} ions increased. SBF solution was used to test the bioactivity of materials for 14 days at 37 °C. The results shows that incorporating Cr^{3+} ions accelerated the degradation rate of βTCP and enhanced the deposition rate of the apatite layer. The antibacterial study of βTCP doped with Cr^{3+} ions confirmed that the samples were effective as antibacterial agents against Pseudomonas aeruginosa (P. aeruginosa).

INTRODUCTION

Nanomaterials exhibit unique traits in structural, chemical, and biological properties. Biomedical researchers may use these materials for various purposes, including tissue engineering, gene delivery, cancer therapy, neurodegenerative disease treatment, inflammatory treatment, and many others. Despite the fact that bionanomaterials are biocompatible, safety toxicity, and regulation remain significant concerns in both research and the marketplace. However, current research has become more structured and has broadened its scope.

In recent decades, ceramic materials have positively impacted human well-being. Bone grafts are utilized to replace or repair damaged or deteriorated skeletal tissues. More than 50 % (by volume) of nanoceramic materials have defects such as interphase boundaries, grain boundaries, and dislocations, which significantly influence the material's physical and chemical properties and their biological interaction with tissues [1, 2]. So far, the calcium phosphate (CaP) ceramic group has gotten the most interest for its potential use in different biological applications, including dentistry and medication administration. CaP ceramics have significantly improved biological affinity and activity with regard to surrounding host tissues. It has been found that CaP ceramics such as β-tricalcium phosphate (βTCP) have a high biological response to physiological conditions [3, 4].

βTCP is a biocompatible and bioactive substitute material used by orthopedic surgeons to promote bone healing. In animal experiments, pure βTCP has significantly improved bone healing compared to nano-structured carbon implants and porous titanium [5]. Another study found that βTCP alone might significantly improve bone regeneration more than bone autografts [6, 7]. βTCP materials may be synthesized using various

chemical materials, followed by conventional heating, such as solid-state and wet chemical precipitation [8, 9]. Conventional heating is expensive and produces impure products due to poor heating, resulting in a longer processing time [10]. Moreover, in traditional heating, the temperature remains non-uniform, which furnishes inferior quality products. The Microwave (MW) assisted wet-precipitation method is another method that has recently been used to synthesize βTCP [11]. For this reason, the heating mechanism of the MW method is much better. Heat energy can be transferred uniformly to the materials [12].

βTCP materials have gained a lot of interest for their use as bone-void fillers to regulate dead space and encourage bone development. Indeed, bioresorbable βTCP with antibacterial properties has been developed because implants, including βTCP become potential sources of bacterial infection [11, 13]. To prevent the contamination of βTCP, different dosages of Ag, Cu, Zn ions have been incorporated into the crystal structure of βTCP to inhibit the growth of a wide range of bacteria [14, 15]. Among the necessary trace elements is trivalent chromium (Cr^{3+}). Diabetic patients benefit from chromium picolinate, an extremely popular dietary supplement, since it helps manage blood sugar levels and lowers heart disease and metabolic syndrome risk factors [16-18]. Chromium-substituted spinel copper ferrite was synthesized by Ansari et al. and tested against *Escherichia coli* (E. coli) in a laboratory environment for antibacterial activity. According to their findings, the antibacterial activity of ferrite nanoparticles rises as the Cr^{3+} ions content increases from 0.0 to 0.4, 0.6, 0.8, 1.0 mole [19].

This study has modified the internal structure βTCP by adding Cr^{3+} ions to improve bioactivity and antibacterial properties. The impact of the addition of Cr^{3+} ions is investigated. The *in vitro* bioactivity was analysed using simulated body fluid (SBF), and antibacterial effectiveness was determined using a disk diffusion assay against standard *Pseudomonas aeruginosa* (P. aureus). Our findings shed light on the true potential of Cr-βTCP micro/nano-granules as promising biomaterials.

EXPERIMENTAL

Calcium nitrate tetrahydrate $Ca(NO_3)_2{\cdot}4H_2O$, diammonium hydrogen phosphate $(NH_4)_2(HPO_4)$, and chromium(III) nitrate $Cr(NO_3)_3$ were used as a source of Ca^{2+}, PO_4^{3-} and Cr^{3+} ions, respectively.

A microwave-wet precipitation method was used to synthesize Cr-βTCP materials. In 100 mL of distilled water, 0.9 mole of $Ca(NO_3)_2$ and x mole of $Cr(NO_3)_3$ were dissolved, and 0.6 mole of $((NH_4)_2HPO_4)$ was poured in drop by drop while being constantly stirred. The pH was set to 9 using NH_4OH, and the precipitation was microwaved for 15 mins at 800W. Subsequently, the residue was allowed to dry at 80 °C for 17 h before being calcined for 2 h at 1200 °C to produce βTCP. The addition amount of Cr^{3+} ions (x) were 0.2, 0.6, 1.0 moles and the samples were labelled as (0.2)Cr-βTCP, (0.6)Cr-βTCP, and (1.0)Cr-βTCP, respectively.

To determine the purity of phases and the lattice parameters of materials, XRD was used. Using a 0.02° step interval and a 1 step/s step length, the diffractogram was recorded at the 20° – 80° ambient temperature range. The morphology and chemical content were investigated (FESEM attached with EDX, Zeiss-LEO Model 1530). Image J software was used to measure the diameters of the particles (National Institutes of Health, USA, 1.47 V).

Before conducting the *in vitro* bioactivity and antibacterial tests, the powdered materials (350 mg) were uniaxially pressed into disks shape (14 mm x 1 mm) using an Instron universal testing machine [INSTRON-600 KN (model 600DX)] at a 35 kN load.

In vitro bioactivity was evaluated using SBF according to the instructions given by Kokubo and Takadama [20]. The compressed disks (350 mg) were soaked in 50 mL of SBF for up to 14 days at 37 °C. A combination of distilled water and ethanol was used to clean the disks after they were carefully removed from the SBF solution and then allowed to dry at lab temperature. Apatite layer shape was studied using FESEM, and the Ca/P ratio of the apatite layer was evaluated with EDX. The concentration of leached Cr^{3+} ions in the filtrate was measured using ICP-MS (Perkin Elmer Sciex, Elan 6100).

Pseudomonas aeruginosa (P. aeruginosa, DSM 50071 strains) was used to assess the antibacterial properties of Cr^{3+} doped βTCP materials using the disk diffusion technique. A 1.0 mL of a bacterial solution containing about 10^5 CFUs/mL bacteria was injected into nutrient agar plates. The disks were put on the inoculation plates and then cultured at 37 °C for 24 h.

RESULTS AND DISCUSSION

The crystal structure analysis of the prepared materials was evaluated using XRD. The results are illustrated in Figure 1. βTCP crystalline diffractograms showed sharp peaks that matched the standard pattern of βTCP (PDF No: 09-0169). The XRD patterns of (0.2)Cr-TCP and (0.6)Cr-TCP showed significant peak widening and reduction in peak intensity, demonstrating that the low incorporation amount of Cr^{3+} ions in the structure reduces the degree of crystallinity of βTCP [21, 22]. However, it increased its crystallinity by incorporating a high amount of Cr^{3+} ions ((1.0)Cr-βTCP). This behaviour could be attributed to substituting Ca^{2+} ions for Cr^{3+} at the 9-coordinated position M (4) [23]. Increased concentrations of Cr^{3+} ions reduced lattice parameters a = b and c. At the same time, the diffraction

peaks moved to higher 2θ values, showing contraction of the lattice parameter when smaller Cr^{3+} ions (0.069 nm) were substituted for bigger Ca^{2+} (0.099 nm) ions in the βTCP structure. [21] (Table 1).

Table 1. Crystal structure of Cr-βTCP materials.

Sample ID	Lattice Parameters			Degree of Crystallinity
	a (Å)	c (Å)	Cell Volume (Å3)	
Standard βTCP	10.429	37.380	3507.34	---
(0.2)Cr-βTCP	10.378	37.228	3472.12	79 %
(0.6)Cr-βTCP	10.365	37.324	3472.56	76 %
(1.0)Cr-βTCP	10.440	37.160	3507.34	83 %

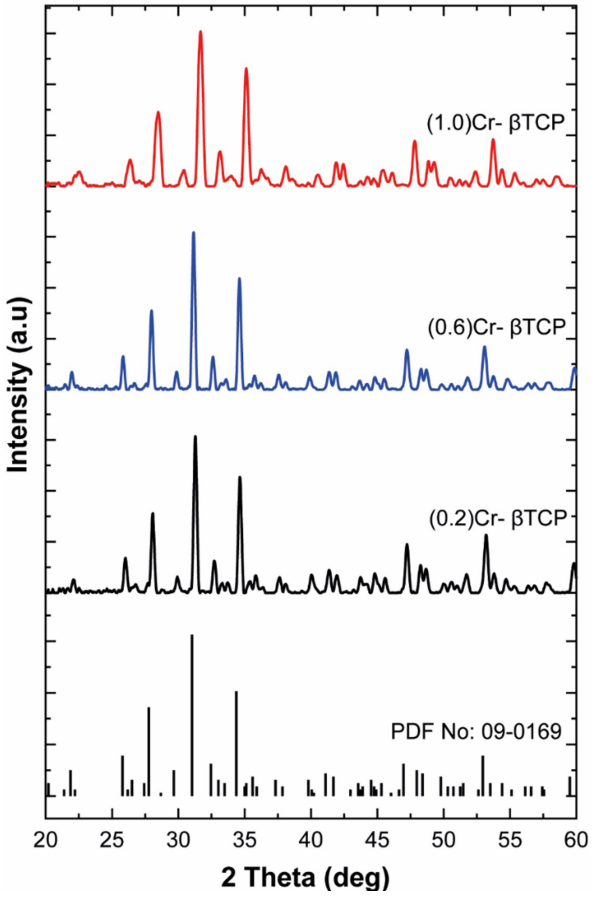

Figure 1. XRD Patterns of the Cr-βTCP series were calcined at 1200 °C for 2 h.

Figure 2 depicts the spherical particle form of Cr-βTCP materials. There were no significant changes in the results as the concentration of Cr^{3+} ions increased. The particle size of (0.2)Cr-βTCP, (0.6)Cr-βTCP, and (1.0)Cr-βTCP were 998 nm, 884 nm, and 1178 nm, respectively. The addition of Cr^{3+} ions enhanced the growth rate of βTCP particles. This behaviour could be attributed to a higher degree of crystallinity, which gradually increased with the incorporation of Cr^{3+} ions.

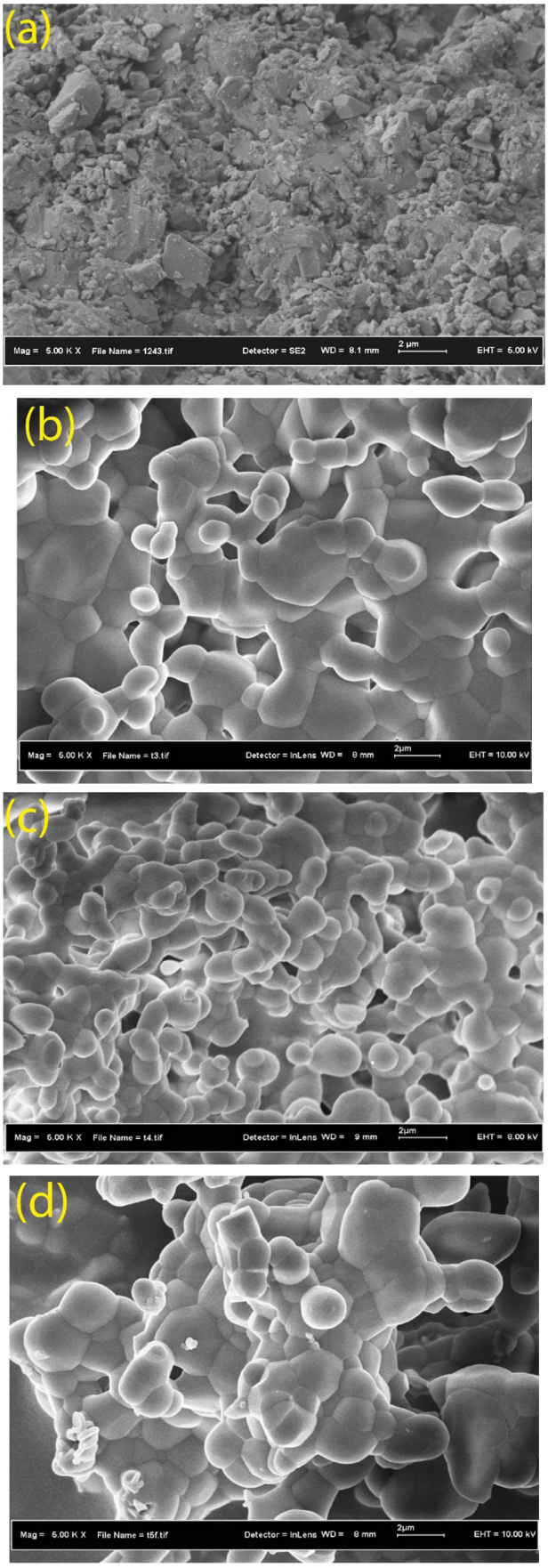

Figure 2. FESEM images of (a) pure βTCP, (b) (0.2)Cr-βTCP, (c) (0.6)Cr-βTCP, and (d) (1.0)Cr-βTCP materials.

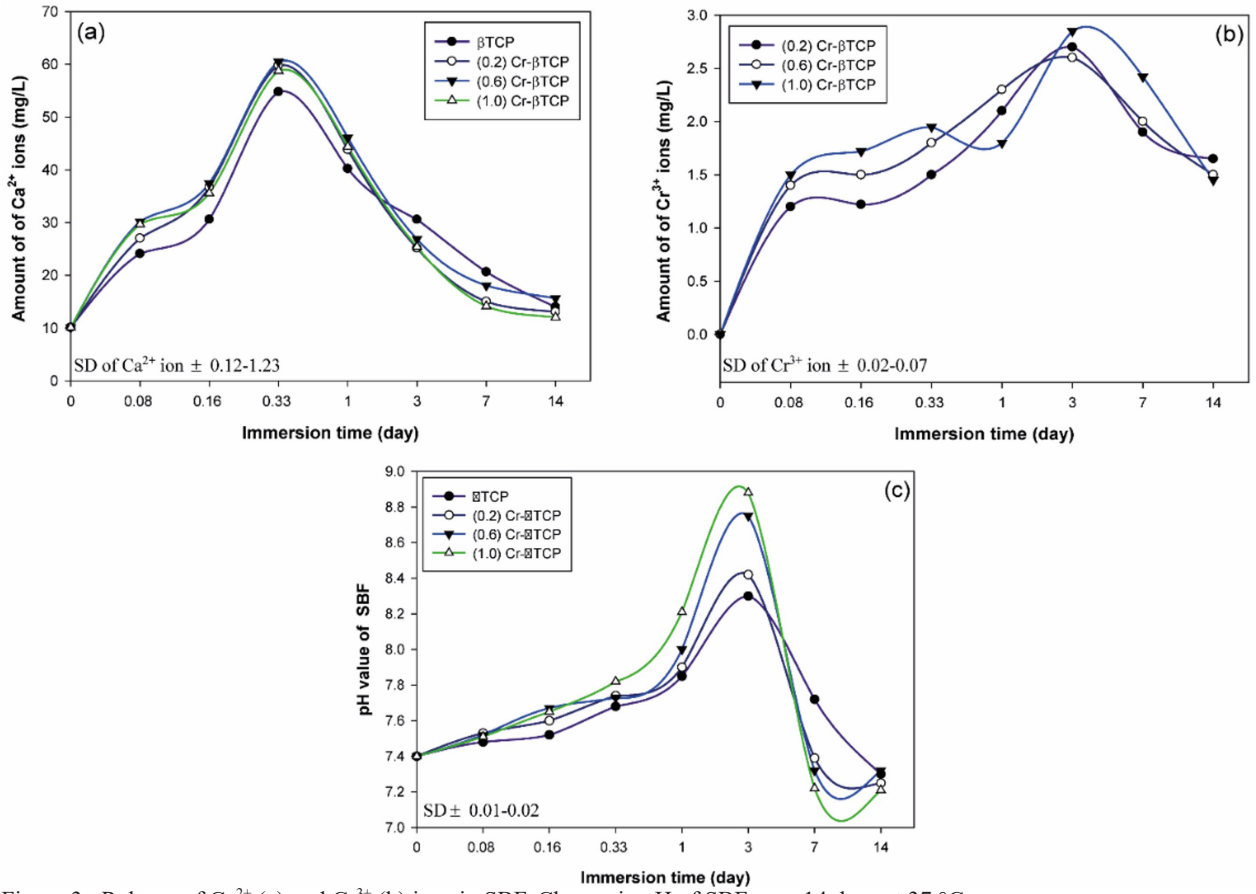

Figure 3. Release of Ca^{2+} (a) and Cr^{3+} (b) ions in SBF. Change in pH of SBF over 14 days at 37 °C.

Table 2. Ca/P ratio of apatite layer.

Samples ID	3 days		7 days		14 days	
	Ca/P	Ca+Cr/P	Ca/P	Ca+Cr/P	Ca/P	Ca+Cr/P
βTCP	1.59	---	1.57	---	1.56	---
(0.2)Cr- βTCP	1.60	1.62	1.64	1.66	1.59	1.60
(0.6)Cr- βTCP	1.63	1.64	1.64	1.65	1.61	1.62
(1.0)Cr- βTCP	1.66	1.68	1.65	1.66	1.64	1.65

SD ± 0.01 – 0.07

The graph (Figure 3a, b) depicts the variation in the Ca^{2+} and Cr^{3+} ions released in the SBF solution. It can see that the dissolution of βTCP and Cr-βTCP samples began rapidly after being soaked in the SBF solution. During the first few hours of the experiment, a progressive rise in the quantity of Ca^{2+} and Cr^{3+} ions released in the SBF solution was recorded. The highest release of Ca^{2+} ions was found after 8 h, but the maximum release of Cr^{3+} ions was observed after 3 days of incubation. With a prolonged incubation period, the amount of Ca^{2+} and Cr^{3+} ions in SBF decreased gradually, linked to the fact that they were consumed during the creation of the apatite layer. Figure 3c displays the change in pH of SBF during Cr-βTCP sample immersion. The pH of the solution first rose, which was attributed to the exchange of Cr^{3+} and Ca^{2+} from the sample surfaces with H^+ from SBF. After the first 3 days, the pH gradually fell due to reduced ion release from the surface of the samples and OH consumption in the formation of the apatite layer.

Figure 4 depicts the growth of an apatite layer on the outside of the Cr-βTCP disks during immersion in SBF for 14 days. After just 3 days of soaking in SBF, the samples' surfaces were layered with tightly packed granules. After 14 days of immersion, the growth became more intense. The number and the size of these granules were augmented with an increase in Cr^{3+} amount, indicating that the Cr^{3+} ion favours the growth of apatite particles.

Apatite layer EDX analysis revealed the existence of Ca, P, and O as the primary apatite layer constituents, while the Ca+Cr/P ratio ranged between 1.56 and 1.68, which is extremely near to the Ca/P ratio of synthetic HA (Table 2).

No antibacterial activity was observed in the case of pure βTCP. However, inhibition zones of 3.1, 7.2,

and 9.3 mm were observed for (0.2)Cr-βTCP, (0.6)Cr-βTCP, and (1.0)Cr-βTCP, respectively (Figure 5). Agar plates show the accumulation of electronegative charges on the cell surface, which acts as nucleation sites for releasing Cr^{3+} ions on the agar plates. These Cr^{3+} ions have the capability to enter the lipid membrane and thus may create disorder in the respiratory system of the cell and further inhibit protein synthesis.

Nevertheless, the mechanisms by which Cr^{3+} ions exert their antibacterial activity are not yet entirely understood. However, earlier research has identified three distinct antibacterial action modalities [24], (i) Cr^{3+} ions penetrate bacteria's cells during an attack and interfere with the formation of intracellular Adenosine Triphosphate (ATP), as well as with DNA replication, (ii) ions may build up in bacteria's cell membrane,

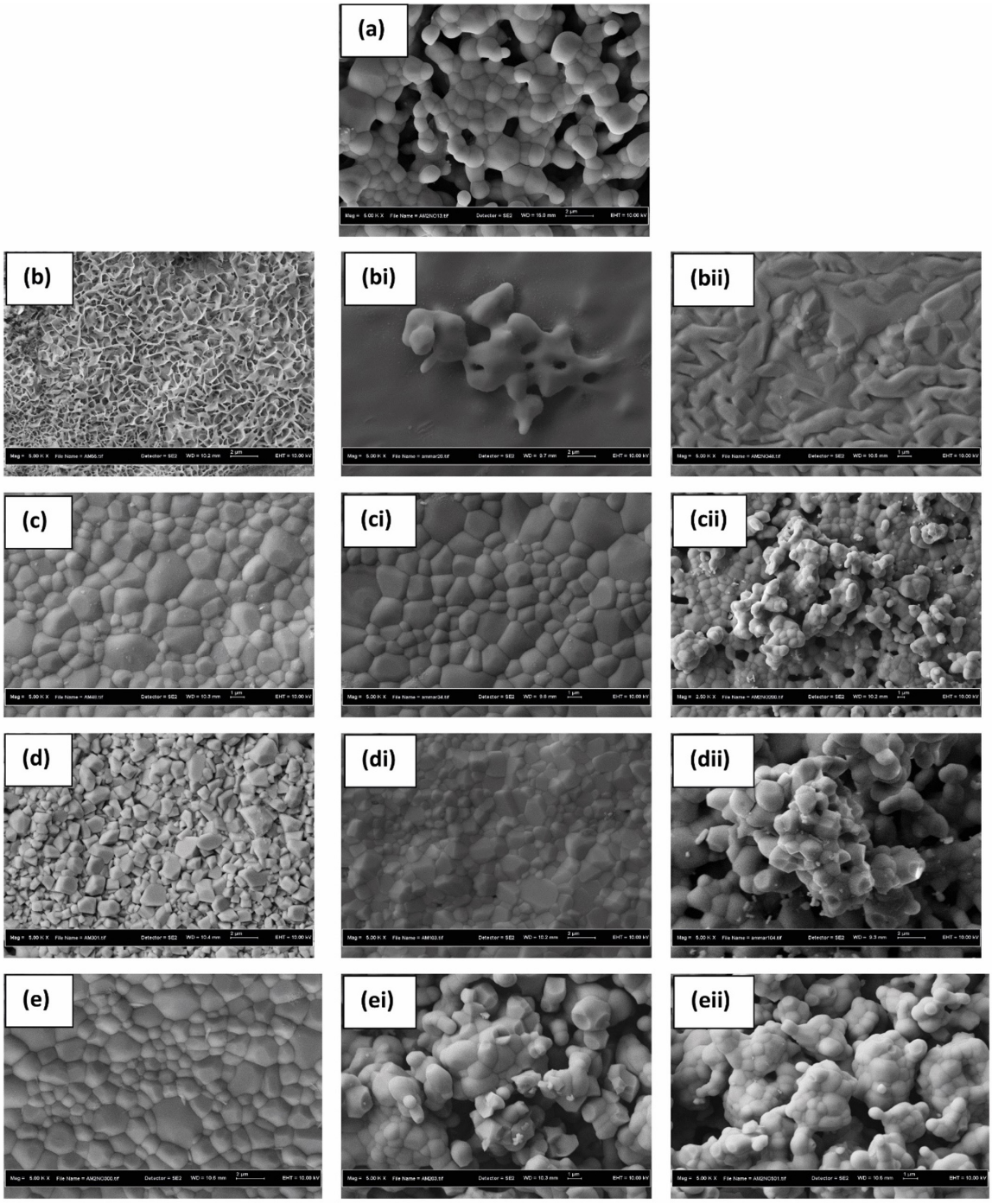

Figure 4. FESEM images of (a) (1.0)Cr-βTCP before soaking in SBF, (b, bi and bii) for βTCP at immersion time 3, 7 and 14 days, respectively, (c, ci and cii) for (0.2)Cr-βTCP at immersion time 3, 7 and 14 days respectively, (d, di and dii) for (0.6)Cr-βTCP at immersion time 3, 7 and 14 days respectively, (e, ei and eii) for (1.0)Cr-βTCP at immersion time 3, 7 and 14 days respectively.

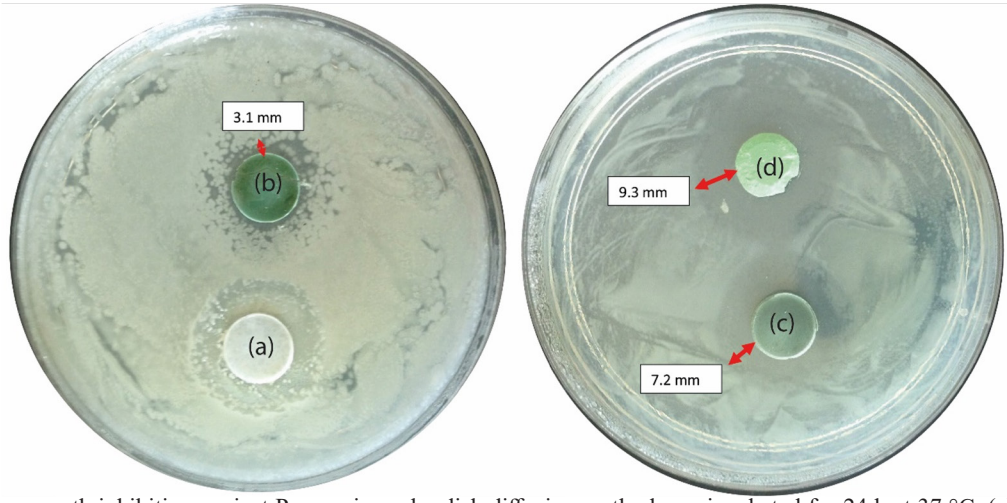

Figure 5. The growth inhibition against P. aeruginosa by disk diffusion method was incubated for 24 h at 37 °C. (a) pure βTCP, (b) (0.2) Cr-βTCP, (c) (0.6) Cr-βTCP, and (d) (1.0) Cr-βTCP materials.

causing changes in permeability (the slow release of proteins and lipopolysaccharides), and transportation of protons across the cell membrane is not allowed, destroying the cell membrane and the death of the bacterial cell, (iii) generation of reactive oxygen radicals, which may react with the membrane, cell wall, and mitochondria of bacteria, eventually destroying the bacterial cells.

CONCLUSIONS

Using a microwave-assisted wet precipitation method, we successfully incorporated different dosages of Cr^{3+} ions into βTCP lattice. Cr^{3+} ions doping increased crystallinity and accelerated crystallite formation, resulting in a more crystallized material. FESEM analysis revealed that incorporating Cr^{3+} enhanced the growth rate of βTCP particles. Cr^{3+} doped βTCP with an additional amount of Cr^{3+} showed the good formation of apatite layer and resistance against P. aeruginosa strain.

Acknowledgments

Dr. Ammar Z. Alshemary would like to thank Al-Mustaqbal University College.

REFERENCES

1. Ur Rehman I. (2004): Nano bioceramics for biomedical and other applications. *Materials Technology, 19*, 224-233. doi: 10.1080/10667857.2004.11753089
2. Catledge S. A., Fries M. D., Vohra Y. K., Lacefield W. R., Lemons J. E., Woodard S., Venugopalanc, R. (2002): Nanostructured ceramics for biomedical implants. *Journal of Nanoscience and Nanotechnology, 2*, 293-312. doi: 10.1166/jnn.2002.116
3. Kivrak, N., and Taş, A. C. (1998): Synthesis of calcium hydroxyapatite-tricalcium phosphate (HA-TCP) composite bioceramic powders and their sintering behavior. *Journal of the American Ceramic Society, 81*, 2245-2252. doi: 10.1111/j.1151-2916.1998.tb02618.x
4. Bow J.-S., Liou S.-C., Chen S.-Y. (2004): Structural characterization of room-temperature synthesized nano-sized β-tricalcium phosphate. *Biomaterials, 25*, 3155-3161. doi: 10.1016/j.biomaterials.2003.10.046
5. Gilev M., Bazarny V., Volokitina E., Polushina L., Maksimova A. Y., Kazakova Y. E. (2019): Laboratory Monitoring of Bone Tissue Remodeling after Augmentation of Impression Intraarticular Fracture with Different Types of Bone Graft. *Bulletin of Experimental Biology and Medicine,167*, 681-684. doi: 10.1007/s10517-019-04598-7
6. Lu H., Zhou Y., Ma Y., Xiao L., Ji W., Zhang Y., Wang X. (2021): Current application of beta-tricalcium phosphate in bone repair and its mechanism to regulate osteogenesis. *Frontiers in Materials, 277*. doi: 10.3389/fmats.2021.698915
7. Pereira R., Gorla L., Boos F., Okamoto R., Júnior I. G., Hochuli-Vieira E. (2017): Use of autogenous bone and beta-tricalcium phosphate in maxillary sinus lifting: histomorphometric study and immunohistochemical assessment of RUNX2 and VEGF. *International Journal of Oral and Maxillofacial Surgery, 46*, 503-510. doi: 10.1016/j.ijom.2017.01.002
8. Ghosh R., Sarkar R. (2016): Synthesis and characterization of sintered beta-tricalcium phosphate: A comparative study on the effect of preparation route. *Materials Science and Engineering: C, 67*, 345-352. doi: 10.1016/j.msec.2016.05.029
9. Boanini E., Gazzano M., Nervi C., Chierotti M. R., Rubini K., Gobetto R., Bigi A. (2019): Strontium and zinc substitution in β-tricalcium phosphate: An X-ray diffraction, solid state NMR and ATR-FTIR study. *Journal of Functional Biomaterials, 10*, 20. doi: 10.3390/jfb10020020
10. Komarneni S., Roy R., Li Q. (1992): Microwave-hydrothermal synthesis of ceramic powders. *Materials Research Bulletin, 27*, 1393-1405. doi: 10.1016/0025-5408(92)90004-J
11. Saleh A. T., Ling L. S., Hussain R. (2016): Injectable magnesium-doped brushite cement for controlled drug release application. *Journal of Materials Science, 51*, 7427-7439. doi: 10.1007/s10853-016-0017-2

12. Kharissova O. V., Kharisov B. I., Valdés J. J. R. (2010): The use of microwave irradiation in the processing of glasses and their composites. *Industrial & Engineering Chemistry Research, 49*, 1457-1466. doi: 10.1021/ie9014765
13. Fadeeva I. V., Lazoryak B. I., Davidova G. A., Murzakhanov F. F., Gabbasov B. F., Petrakova N. V., Fosca M., Barinov S. M., Vadalà G., Uskoković V., Zheng Y., Rau J. V. (2021): Antibacterial and cell-friendly copper-substituted tricalcium phosphate ceramics for biomedical implant applications. *Materials Science and Engineering: C, 129*, 112410. doi: 10.1016/j.msec.2021.112410
14. Yuan J., Wang B., Han C., Huang X., Xiao H., Lu X., Lu J., Zhang D., Xue F., Xie Y. (2020): Nanosized-Ag-doped porous β-tricalcium phosphate for biological applications. *Materials Science and Engineering: C, 114*, 111037. doi: 10.1016/j.msec.2020.111037
15. Jacobs A., Renaudin G., Charbonnel N., Nedelec J.-M., Forestier C., Descamps S. (2021): Copper-Doped Biphasic Calcium Phosphate Powders: Dopant Release, Cytotoxicity and Antibacterial Properties. *Materials, 14*, 2393. doi: 10.3390/ma14092393
16. Paiva A. N., Lima J. G. d., Medeiros A. C. Q. d., Figueiredo H. A. O., Andrade R. L. d., Ururahy M. A. G., Rezende A. A., Brandão-Neto J., Almeida M. d. G. (2015): Beneficial effects of oral chromium picolinate supplementation on glycemic control in patients with type 2 diabetes: A randomized clinical study. *Journal of Trace Elements in Medicine and Biology, 32*, 66-72. doi: 10.1016/j.jtemb.2015.05.006
17. Albarracin C., Fuqua B., Geohas J., Juturu V., Finch M. R., Komorowski J. R. (2007): Combination of chromium and biotin improves coronary risk factors in hypercholesterolemic type 2 diabetes mellitus: a placebo-controlled, double-blind randomized clinical trial. *Journal of the Cardiometabolic Syndrome, 2*, 91-97. doi: 10.1111/j.1559-4564.2007.06366.x
18. Rentsch B., Bernhardt A., Henß A., Ray S., Rentsch C., Schamel M., Gbureck U., Gelinsky M., Rammelt S., Lode A. (2018): Trivalent chromium incorporated in a crystalline calcium phosphate matrix accelerates materials degradation and bone formation in vivo. *Acta biomaterialia, 69*, 332-341. doi: 10.1016/j.actbio.2018.01.010
19. Ansari M.A., Baykal A., Asiri S., Rehman S. (2018): Synthesis and characterization of antibacterial activity of spinel chromium-substituted copper ferrite nanoparticles for biomedical application. *Journal of Inorganic and Organometallic Polymers and Materials, 28*, 2316-2327. doi:10.1007/s10904-018-0889-5
20. Kokubo, T., and Takadama, H. (2006): How useful is SBF in predicting in vivo bone bioactivity? *Biomaterials, 27*, 2907-2915. doi: 10.1016/j.biomaterials.2006.01.017
21. Wakamura M., Kandori K., Ishikawa T. (1997): Influence of chromium(III) on the formation of calcium hydroxyapatite. *Polyhedron, 16*, 2047-2053. doi: 10.1016/S0277-5387(96)00513-X
22. M. Sallam S. (2012): Synthesis and characterization of hydroxyapatite contain chromium. *Journal of Biophysical Chemistry, 03*, 278-282. doi: 10.4236/jbpc.2012.34033
23. Enderle R., Götz-Neunhoeffer F., Göbbels M., Müller F. A., Greil P. (2005): Influence of magnesium doping on the phase transformation temperature of β-TCP ceramics examined by Rietveld refinement. *Biomaterials, 26*, 3379-3384. doi: 10.1016/j.biomaterials.2004.09.017
24. Alshemary A. Z., Sarsık B., Salman N. A., Şahin S. M., Şahin M. M., Muhammed Y. (2022): Evaluation of Antibacterial Activity of Calcium Phosphates Based Bone Cements for Biomedical Applications. *Egyptian Journal of Chemistry, 65*, 5-6. doi: 10.21608/EJCHEM.2021.110005.5013